

Article

Silver(I)-Catalyzed C4-H Amination of 1-Naphthylamine Derivatives with Azodicarboxylates at Room Temperature

Yuxue Zhang [†], Mengxue Pei [†], Fan Yang ^{*} and Yangjie Wu

College of Chemistry, Green Catalysis Center, Henan Key Laboratory of Chemical Biology and Organic Chemistry, Key Laboratory of Applied Chemistry of Henan Universities, Zhengzhou University, Zhengzhou 450052, China

^{*} Correspondence: yangf@zzu.edu.cn

[†] These authors contributed equally to this work.

Abstract: A highly facile and efficient protocol for silver(I)-catalyzed C4-H amination of 1-naphthylamine derivatives with readily available azodicarboxylates utilizing picolinamide as a bidentate directing group is reported, providing an alternative strategy for the synthesis of 4-aminated 1-naphthylamine derivatives. The reaction proceeded smoothly in acetone at room temperature undergoing a self-redox process under the base and external oxidant-free conditions, affording the desired products with good to excellent yields.

Keywords: C-H activation; 1-naphthylamine derivatives; amination; silver catalysis; azodicarboxylates



Citation: Zhang, Y.; Pei, M.; Yang, F.; Wu, Y. Silver(I)-Catalyzed C4-H Amination of 1-Naphthylamine Derivatives with Azodicarboxylates at Room Temperature. *Catalysts* **2022**, *12*, 1006. <https://doi.org/10.3390/catal12091006>

Academic Editors: Antonia Iazzetti and Alessia Ciogli

Received: 18 August 2022

Accepted: 30 August 2022

Published: 6 September 2022

Publisher's Note: MDPI stays neutral with regard to jurisdictional claims in published maps and institutional affiliations.



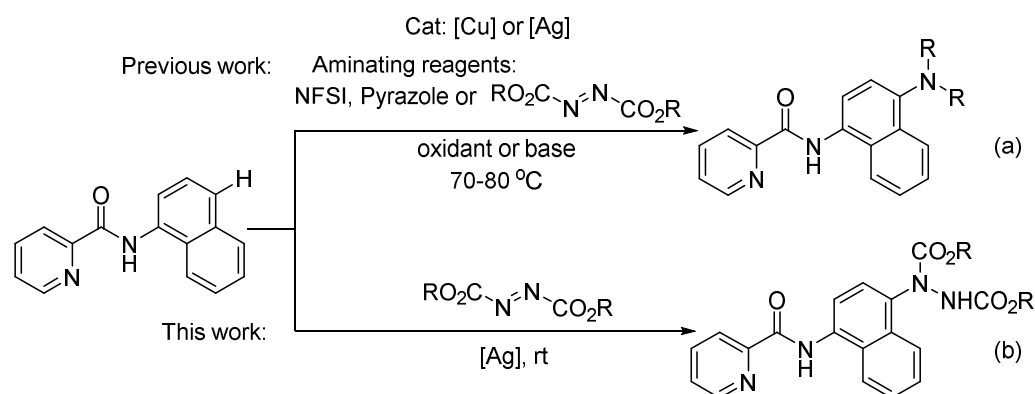
Copyright: © 2022 by the authors. Licensee MDPI, Basel, Switzerland. This article is an open access article distributed under the terms and conditions of the Creative Commons Attribution (CC BY) license (<https://creativecommons.org/licenses/by/4.0/>).

1. Introduction

Arylamine compounds are important structural fragments in pharmaceuticals, agrochemicals, dyes, herbicides, and functionalized materials [1–3]. Therefore, the development of efficient methods for C–N bond construction have captured much attention. However, traditional synthesis methods usually use pre-functionalized substrates as raw materials to achieve the synthesis of target products, which will increase the cost of reaction synthesis and the complexity of experimental operations [4,5].

In the past few decades, the transition metal-catalyzed C–H functionalization has emerged as a reliable tool in organic synthesis [6–12]. Therefore, direct oxidative cross-dehydrogenative-coupling (CDC) amination of hydrocarbons with amines has gradually become a fascinating protocol for the C–N bond-forming reaction due to its atom- and step-economy. In 2005, Daugulis' group introduced a type of picolinamide (PA) moiety as a directing group to complete the C–H activation process, [13] and then, a series of reports for C2–H [14–21] and C8–H [22–29] functionalization reactions of 1-naphthylamine derivatives started to appear. Remarkably, different kinds of C4–H functionalization of 1-naphthylamides derivatives were developed, such as sulfonylation, [30–32] amination, [33–37] esterification, [38,39] etherification [40]. Among them, the traditional transition metal-catalyzed amination reaction of 1-naphthylamine derivatives at the C4 site usually utilizes a stoichiometric amount of base and oxidant under heated conditions, and the reaction cost is relatively higher (Scheme 1a).

In recent years, the research interest in our group has mainly focused on the regioselective C–H functionalization of arene compounds with the assistance of the bidentate directing group, such as the direct C–H functionalization of 1-naphthylamine derivatives [24,29,31,33,36,37] and 8-aminoquinoline derivatives [41–44]. Especially in 2018, our research group reported the reaction of 1-naphthylamine derivatives and azodicarboxylates and successfully realized the C4–H bond amination of the 1-naphthylamine derivative [33]. In this work, we would like to report a facile and efficient protocol for the C4–H amination of 1-naphthylamine derivatives with azodicarboxylates at room temperature under base and oxidant-free conditions (Scheme 1b).



Scheme 1. The C4-H Amination of 1-Naphthylamines. (a) C4-H Amination of 1-Naphthylamines under basic or acidic conditions (b) C4-H Amination of 1-Naphthylamines under basic and acidic-free conditions.

2. Results and Discussion

Initially, N-(naphthalen-1-yl) picolinamide (**1a**) and diisopropyl azodicarboxylate (DIAD, **2a**) was explored as the template reaction substrates for the C4–H amination of 1-naphthylamine derivatives (Table 1 and Tables S1–S3 in Supplementary Materials), and the amination proceeded smoothly in DCE at room temperature in the presence of Ag₂O (10 mol%), resulting in the product **3aa** in an 80% isolated yield (Table 1, entry 1). The reaction solvents were then examined, and the results showed that acetone was the best solvent with a high yield of 97% (Table 1, entries 2–6). Next, some metal catalysts were examined, and none of them could match the catalytic efficiency of Ag₂O (Table 1, entries 7–10). Finally, some control experiments were explored. The reaction did not occur in the absence of Ag₂O, indicating that Ag₂O played an indispensable role in the reaction (Table 1, entry 11), reducing the reaction time or the catalyst loading results in lower yields of the target product (Table 1, entries 12 and 13).

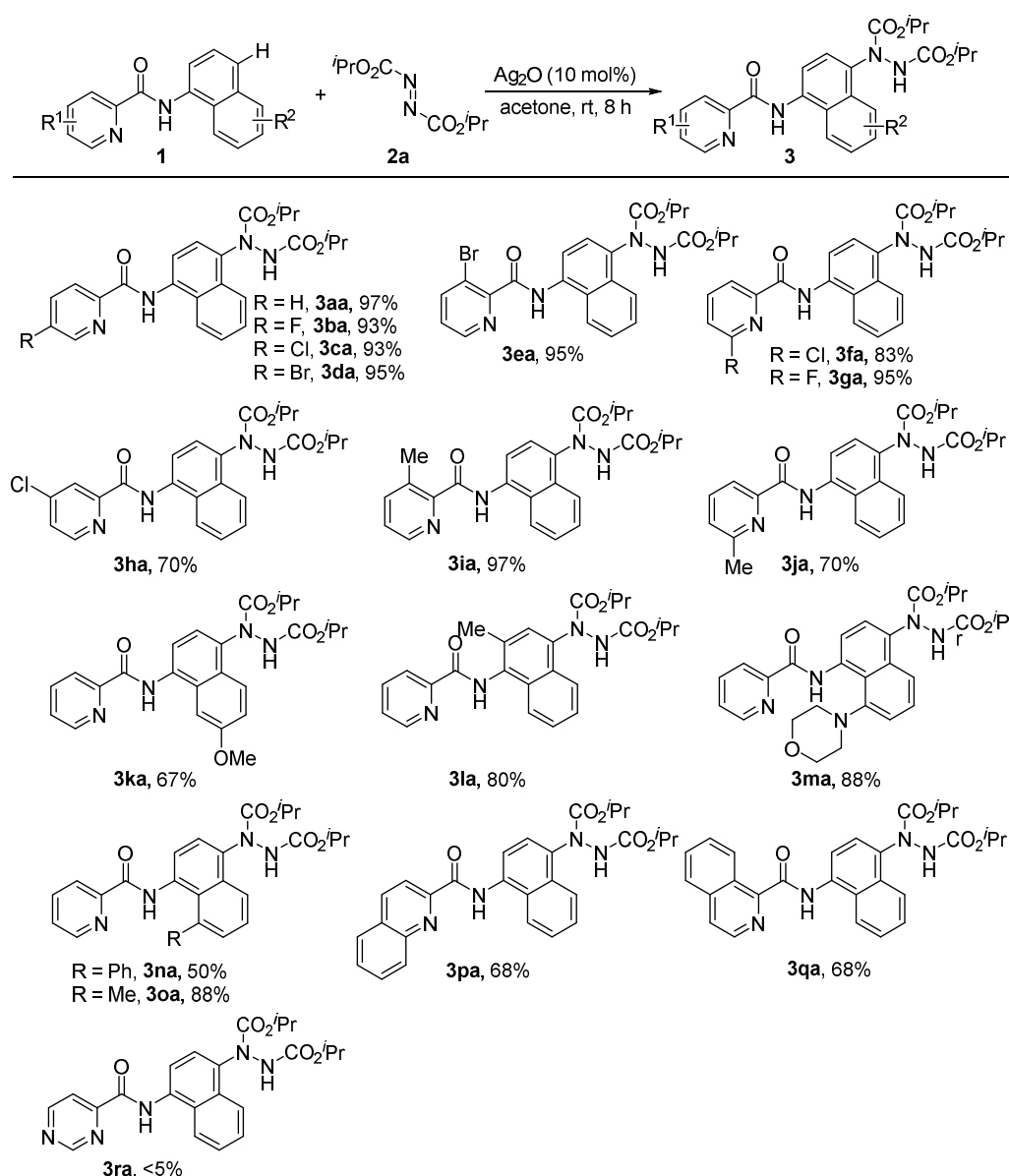
Table 1. Optimization of the reaction conditions ^a.

Entry	Catalyst	Solvent	Yield (%) ^b
1	Ag ₂ O	DCE	80
2	Ag ₂ O	dioxane	90
3	Ag ₂ O	acetone	97
4	Ag ₂ O	THF	90
5	Ag ₂ O	DME	80
6	Ag ₂ O	DCM	<5
7	CuO	acetone	<5
8	Cu ₂ O	acetone	<5
9	Fe ₂ O ₃	acetone	<5
10	AgOAc	acetone	<5
11	-	acetone	<5
12 ^c	Ag ₂ O	acetone	88
13 ^d	Ag ₂ O	acetone	46

^a Reaction conditions: **1a** (0.1 mmol), **2a** (0.2 mmol), catalyst (10 mol%) in solvent (1 mL) at room temperature for 8 h. ^b Isolated yield based on **1a**. ^c For 7 h. ^d With a catalyst loading of 5 mol%.

With the above-optimized reaction conditions, the scope of 1-naphthylamine derivatives was then explored with diisopropyl azodicarboxylate (**2a**), depicted in Scheme 2.

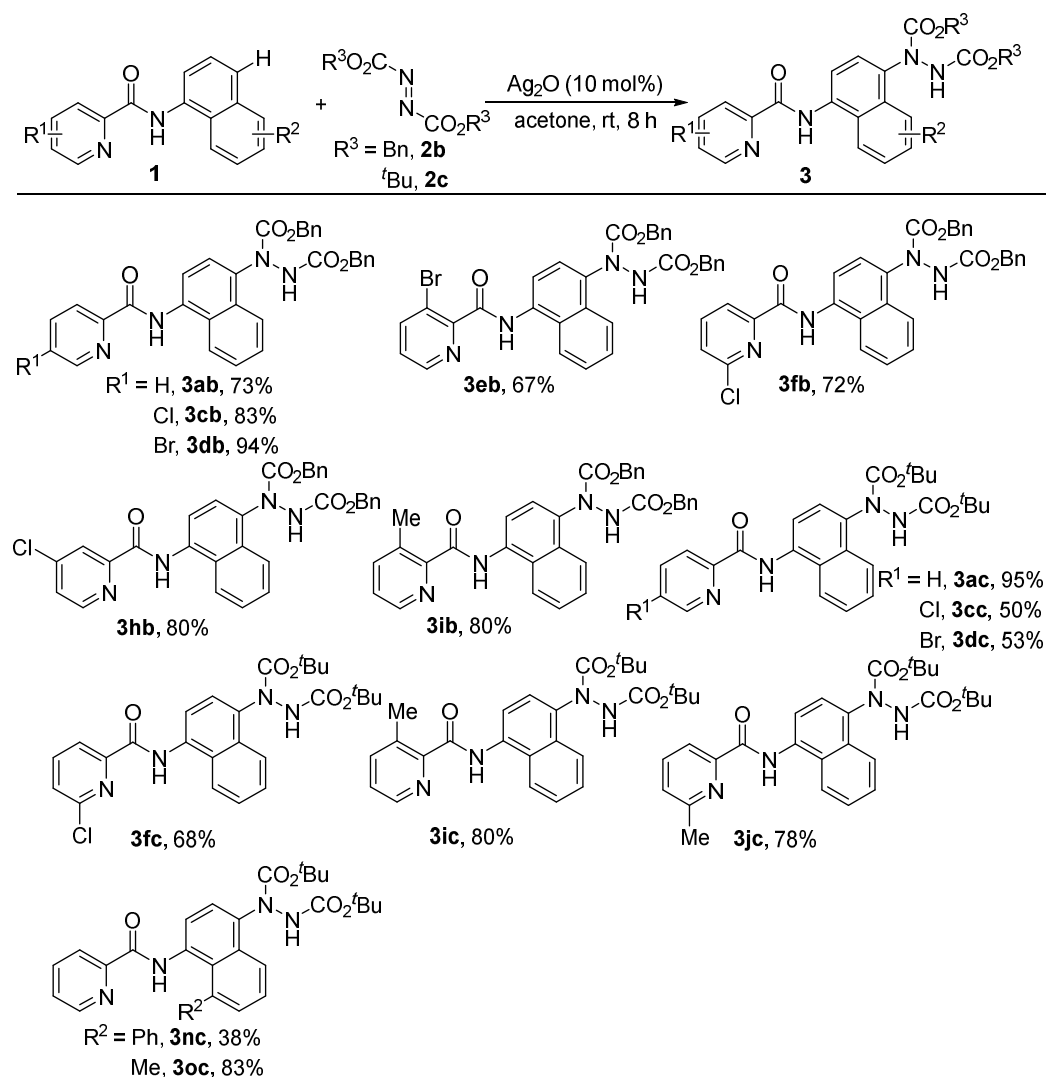
When there was a halogen (F, Cl and Br) substituent at the C3, C4, C5, or C6 position of the pyridine ring of N-(naphthalen-1-yl) picolinamide, the reaction proceeded smoothly to afford the corresponding aminated products in excellent yields (**3ba–3ha**). In the case of the pyridine ring bearing a methyl substituent at the C3 or C6 position, aminated products were obtained in good yields of 97% and 70%, respectively (**3ia** and **3ja**). These results indicate that the pyridine ring of the 1-naphthylamine derivatives could be compatible with the electron-withdrawing and electron-donating groups. When the naphthalene ring of the substrate possesses an electron-donating group at the C2, C7 or C8 position, the reaction could also proceed smoothly to afford products in moderate to good yields (**3ka–3oa**). When a quinoline ring was taken instead of the pyridine ring of the substrate, the reaction could generate the corresponding target product in yields in lower yields of 68% (**3pa** and **3qa**). However, when a pyrimidine ring was utilized as a directing group instead of the pyridine ring, the reaction could not occur at all (**3ra**). These results show that the directing group of 1-naphthylamine derivatives plays an important role in this reaction.



Scheme 2. Substrate Scope of 1-Naphthylamine Derivatives with Diisopropyl Azodicarboxylate (**2a**).

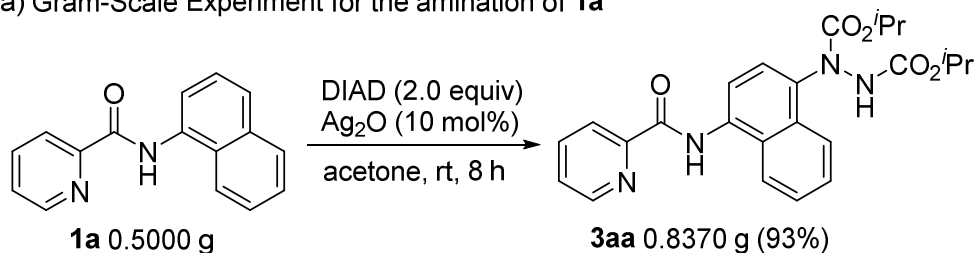
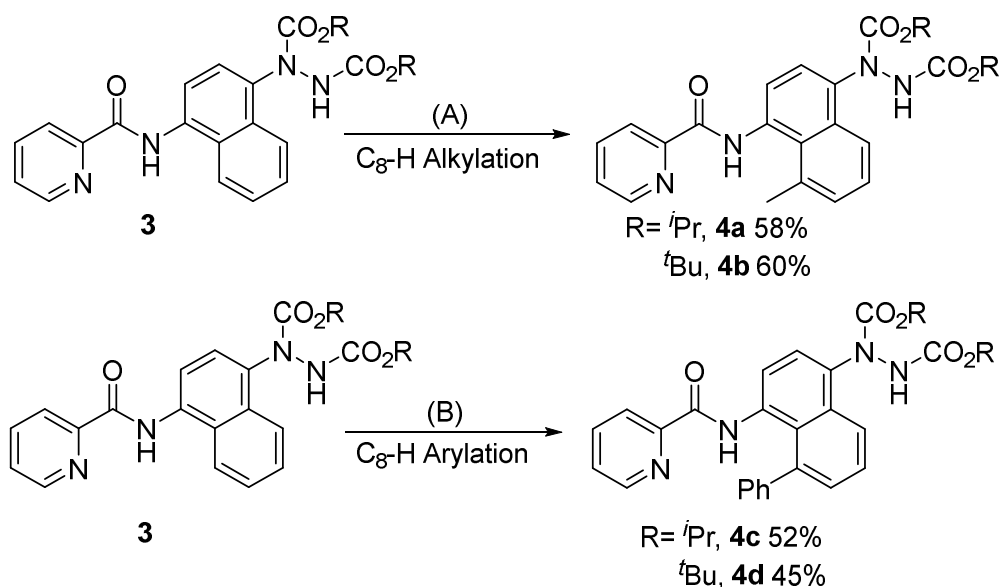
Then, the substrate scope of 1-naphthylamine derivatives with dibenzyl azodicarboxylate (**2b**) or di-*tert*-butyl azodicarboxylate (**2c**) was also screened, and the results are

summarized in Scheme 3. The pyridine ring of 1-naphthylamine derivatives could be compatible with functional groups such as halogen atom, methyl and phenyl groups at the C3, C4, C5, or C6 position, leading to the target products in high yields, the results of which are similar to those of Scheme 2. In addition, the naphthalene ring of 1-naphthylamine derivative bearing a phenyl or methyl group at the C8 position reacted with di-*tert*-butyl azodicarboxylate (**2c**) could result in the target products in yields of 38% and 83%, respectively (**3nc** and **3oc**).



Scheme 3. Substrate Scope of 1-Naphthylamine Derivatives with Dibenzyl Azodicarboxylate (**2b**) or Di-*tert*-butyl Azodicarboxylate (**2c**).

In order to explore the applicability of this protocol, synthetic applications of the product were demonstrated (Scheme 4). A gram-scale experiment of **1a** (0.5000 g) and 2.0 equiv. of diisopropyl azodicarboxylate (**2a**) proceeded under standard conditions, affording the product **3aa** (0.8370 g) with a high yield of 93% (Scheme 4a). Subsequently, some useful transformation of product **3** was pursued such as alkylation and arylation of the naphthyl ring at the C8 position, and bi-functionalized products of 1-naphthylamine derivatives were obtained in moderate yields (Scheme 4b).

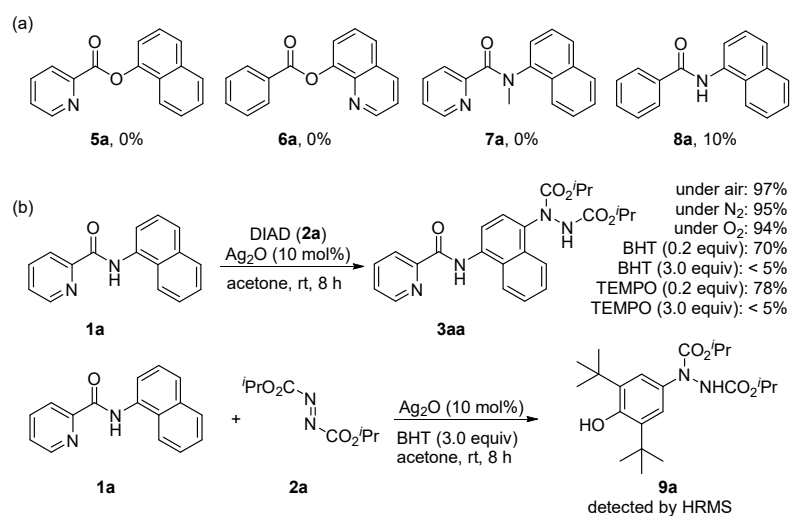
a) Gram-Scale Experiment for the amination of **1a**b) Further alkylation and arylation of Products **3**

Reaction Conditions for A: **3** (0.1 mmol), CH_3I (0.4 mmol), $\text{Pd}(\text{OAc})_2$ (15 mol%), and KOAc (0.2 mmol) in 1,4-dioxane (1.0 mL) at 130 °C for 24 h.

Reaction Conditions for B: **3** (0.1 mmol), PhI (0.4 mmol), $\text{Pd}(\text{OAc})_2$ (15 mol%), and KOAc (0.2 mmol) in xylene (1.0 mL) at 130 °C for 12 h.

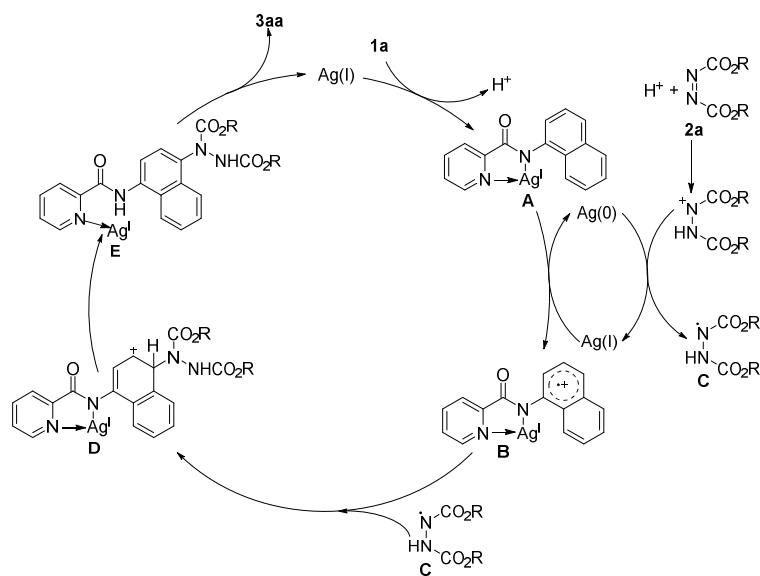
Scheme 4. Synthetic Application. (a) Gram-Scale Experiment for the amination of **1a**. (b) Further alkylation and arylation of Products **3**.

In order to explore the reaction mechanism, some control experiments were investigated (Scheme 5). Some designed substrate analogs pending N, O- or N-chelating groups instead of the N, N-bidentate directing group were conducted in this amination reaction, and the products were obtained in low yields or even no products were observed, indicating that the N, N-bidentate directing group is crucial for this reaction (**5a–8a**). The reaction under a nitrogen and oxygen atmosphere afforded similar yields to that of those performed with air, suggesting that oxygen might not have a very significant effect on this reaction and this reaction might proceed via the self-redox process (Scheme 5b). Then, the 0.2 equiv. radical inhibitor such as 2,2,6,6-tetramethyl-1-piperidinyloxy (TEMPO) or 2,6-di-*tert*-butyl-4-methylphenol (BHT) was added to the amination reaction, and the product **3aa** was obtained in a lower yield; when the loading of TEMPO or BHT increased to 3.0 equiv., the reaction was inhibited successfully; in the presence of BHT under standard conditions, an adduct **9a** of BHT with **2a** was detected by HRMS (Scheme 5b). These results could imply that the reaction might proceed through a radical process.



Scheme 5. Mechanistic Study. (a) Some Substrates Analogues. (b) Effect of Radical Inhibitors on the Reaction.

On the basis of the above-mentioned obtained results and previous reports of [33–37], a plausible mechanism is proposed as shown in Scheme 6. First, N-(naphthalen-1-yl) picolinamide **1a** potentially coordinates with Ag(I) species to afford an aryl-Ag(I) intermediate **A**, the single electron transfer process of which with Ag(I) species occurs to generate an aryl-Ag(I) intermediate radical **B** and Ag(0) species. On the other hand, the electrophilic addition of a proton to the azodicarboxylate **2a** occurs to generate a nitrogen-centered cation, a redox process of which with the Ag(0) species leads to a nitrogen-centered radical **C** and active Ag(I) species to fulfill the Ag(I)/Ag(0) catalytic cycle. Subsequently, the electrophilic attack of the nitrogen-centered radicals **C** to the aryl-Ag(I) intermediate **B** takes place to afford an aryl-Ag(I) intermediate **D**. Finally, the intramolecular proton transfer process of the aryl-Ag(I) intermediate **D** affords the N-Ag(I) coordinated complex **E**, the ligand dissociation of which would result in the target product **3aa** and regenerate catalytically active Ag(I) species to complete the catalytic cycle.



Scheme 6. Possible Pathway.

Intermediate **B** is an open-shell structure with a single unpaired electron distributed in the complex. Mulliken spin densities and singly occupied molecular orbitals (SOMO) are shown in Figure 1. The highest spin density is located on the *para*-carbon atom C4

(0.36 au), followed by a lower spin density on the *ortho*-carbon C2 (0.27 au) in the naphthyl ring. A molecular orbital (MO) analysis showed that the SOMO is primarily located on the naphthyl ring with partial contribution from the core region of N-Ag-N of the intermediate **B**. Among all the carbon atoms in the naphthyl ring, C4 is calculated to be the most-likely reactive site for the attack of the nitrogen radical, which is consistent with experiments.

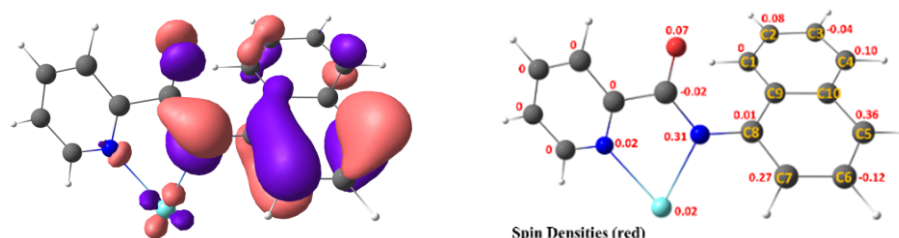


Figure 1. The intermediate **B** was optimized using B3LYP in combination with the LANL2TZ effective core potential (ECP) for Ag, and 6–311G (d, p) for all other atoms. The D3 version of Grimme’s dispersion (GD3) and Truhlar’s SMD solvation model with acetone as the model solvent was adopted for the geometry optimization. Spin densities (red) are in atomic units. The single occupied molecular orbital (SOMO) is depicted with $0.03 \text{ au}^{-3/2}$ isovalue.

3. Experimental Section

3.1. General Information

^1H and ^{13}C NMR spectra were recorded on a Bruker DPX-400 spectrometer with CDCl_3 as the solvent and TMS as an internal standard. Chemical shifts are expressed in parts per million (δ) and the signals were reported as s (singlet), d (doublet), t (triplet), m (multiplet), and coupling constants (J) were given in Hz. Chemical shifts as internal standard were referenced to CDCl_3 ($\delta = 7.26$ for ^1H and $\delta = 77.16$ for ^{13}C NMR as internal standard). Melting points were measured using a WC-1 microscopic apparatus. High-resolution mass spectra were ensured on an Agilent Technologies 1290–6540 HPLC/Accurate-Mass Quadrupole Time-of-Flight LC/MS. All solvents and chemicals were obtained from commercial sources and used as received without further purification unless otherwise noted.

3.2. General Procedure for Synthesis of Product **3aa**

A Schlenk tube was equipped with a magnetic stir bar and charged with N-(naphthalen-1-yl)picolinamide **1a** (0.1 mmol), **2a** (0.2 mmol, 2 equiv), Ag_2O (10 mol%) in acetone (1.0 mL). The resulting mixture was sealed and stirred for 8 h at room temperature. Upon completion, CH_2Cl_2 (10 mL) was added to the reaction system, and the resulting mixture was filtered through a pad of celite. The filtrate was extracted with H_2O (20 mL), and the aqueous layer was extracted with CH_2Cl_2 ($2 \times 10 \text{ mL}$). The collected organic layer was dried with anhydrous Na_2SO_4 , filtered and concentrated under vacuum. The residue was purified by column chromatography on silica gel (200–300 mesh) using hexane-EtOAc as eluent (3:1, *v/v*) to afford the pure product **3aa**.

3.3. General Procedure for Synthesis of Product **3**

Mixture of **3** (0.1 mmol, 1.0 equiv), $\text{Pd}(\text{OAc})_2$ (15 mol%), CH_3I or PhI (0.4 mmol, 4.0 equiv), anhydrous KOAc (0.2 mmol, 2.0 equiv), and 1,4-dioxane or xylene (1 mL) was placed in a 25 mL Schlenk tube with a rubber plug under air. The tube was heated at $130 \text{ }^\circ\text{C}$ for 24 h or 12 h. The reaction mixture was cooled to room temperature, diluted with ethyl acetate, filtered through celite, and concentrated in vacuo. The residue was purified by silica gel column chromatography with petroleum ether-ethyl acetate (5:1, *v/v*) to afford the desired products.

3.4. Spectral Data for Products

3aa. pale yellow solid. (44.0 mg, 97%), $R_f = 0.32$ (25% EtOAc in hexane), mp $176.9\text{--}178.0 \text{ }^\circ\text{C}$; ^1H NMR (400 MHz, CDCl_3) δ 10.82 (s, 1H), 8.71 (d, $J = 7.93 \text{ Hz}$, 1H), 8.36 (d, $J = 7.93 \text{ Hz}$,

1H), 8.36 (d, $J = 7.81$ Hz, 1H), 8.12–8.10 (m, 2H), 7.94 (td, $J_1 = 1.56$ Hz, $J_2 = 7.68$ Hz, 1H), 7.75 (s, 1H), 7.63–7.56 (m, 2H), 7.54–7.51 (m, 1H), 7.28 (s, 1H), 5.02–5.01 (m, 2H), 1.25–1.05 (m, 12H); ^{13}C NMR (100 MHz, CDCl_3) δ 162.2, 156.1, 149.8, 148.1, 137.8, 134.9, 132.7, 130.7, 126.9, 126.8, 126.7, 126.5, 126.0, 123.7, 122.5, 120.8, 118.1, 70.9, 70.0, 22.0, 21.8; HRMS (ESI⁺) m/z [M + H]⁺ calcd for $\text{C}_{24}\text{H}_{27}\text{N}_4\text{O}_5$: 451.1976, Found: 451.1977.

3ba. yellow solid (43.6 mg, 93%), $R_f = 0.32$ (25% EtOAc in hexane), mp 156.5–158.0 °C; ^1H NMR (400 MHz, CDCl_3) δ 10.55 (s, 1H), 8.53 (d, $J = 2.70$ Hz, 1H), 8.40–8.37 (m, 2H), 8.09–8.05 (m, 2H), 7.77–7.75 (m, 1H), 7.64–7.54 (m, 3H), 7.36 (s, 1H), 5.05–5.01 (m, 2H), 1.44–1.09 (m, 12H); ^{13}C NMR (100 MHz, CDCl_3) δ 161.4 (d, $J = 263.43$ Hz), 161.2, 156.1, 146.2 (d, $J = 3.79$ Hz), 136.8 (d, $J = 25.40$ Hz), 135.1, 132.5, 130.7, 126.8 (d, $J = 11.09$ Hz), 126.5, 125.9, 124.5, 124.4, 124.3 (d, $J = 18.66$ Hz), 123.8, 120.7, 118.3, 70.9, 70.0, 22.0; ^{19}F NMR (376 MHz, CDCl_3): δ -121.18 (s, 1F); HRMS (ESI⁺) m/z [M + H]⁺ calcd for $\text{C}_{24}\text{H}_{26}\text{FN}_4\text{O}_5$: 469.1882, Found: 469.1881.

3ca. yellow solid (45.0 mg, 93%), $R_f = 0.32$ (25% EtOAc in hexane), mp 170.9–172.6 °C; ^1H NMR (400 MHz, CDCl_3) δ 10.57 (s, 1H), 8.64 (d, $J = 2.07$ Hz, 1H), 8.38 (d, $J = 7.97$ Hz, 1H), 8.30 (d, $J = 8.36$ Hz, 1H), 8.09–8.04 (m, 2H), 7.91 (dd, $J_1 = 2.31$ Hz, $J_2 = 8.37$ Hz, 1H), 7.76 (s, 1H), 7.62–7.56 (m, 2H), 7.32 (s, 1H), 5.02–5.01 (m, 2H), 1.43–1.09 (m, 12H); ^{13}C NMR (100 MHz, CDCl_3) δ 161.4, 156.1, 148.0, 147.2, 137.5, 135.5, 135.2, 132.4, 130.7, 126.9, 126.8, 126.2, 125.9, 123.8, 123.6, 120.6, 118.3, 70.9, 70.0, 22.0; HRMS (ESI⁺) m/z [M + H]⁺ calcd for $\text{C}_{24}\text{H}_{26}\text{ClN}_4\text{O}_5$: 485.1586, Found: 485.1584.

3da. yellow solid (50.1 mg, 95%), $R_f = 0.32$ (25% EtOAc in hexane), mp 139.5–140.5 °C; ^1H NMR (400 MHz, CDCl_3) δ 10.58 (s, 1H), 8.76 (d, $J = 1.96$ Hz, 1H), 8.38 (d, $J = 7.95$ Hz, 1H), 8.24 (d, $J = 8.30$ Hz, 1H), 8.08–8.04 (m, 3H), 7.75 (s, 1H), 7.62–7.56 (m, 2H), 7.29 (s, 1H), 5.02–5.01 (m, 2H), 1.25–1.09 (m, 2H); ^{13}C NMR (100 MHz, CDCl_3) δ 161.5, 156.1, 149.4, 148.3, 140.5, 135.2, 132.4, 130.7, 126.8, 126.8, 126.6, 125.9, 124.5, 124.0, 123.8, 120.6, 118.3, 70.9, 70.0, 22.0; HRMS (ESI⁺) m/z [M + H]⁺ calcd for $\text{C}_{24}\text{H}_{26}\text{BrN}_4\text{O}_5$: 529.1081, Found: 529.1077.

3ea. yellow solid (50.3 mg, 95%), $R_f = 0.32$ (25% EtOAc in hexane), mp 176.2–178.4 °C; ^1H NMR (400 MHz, CDCl_3) δ 10.74 (s, 1H), 8.64 (dd, $J_1 = 1.00$ Hz, $J_2 = 4.40$ Hz, 1H), 8.40 (d, $J = 7.20$ Hz, 1H), 8.12–8.02 (m, 3H), 7.73 (s, 1H), 7.61–7.59 (m, 2H), 7.35 (dd, $J_1 = 4.53$ Hz, $J_2 = 8.08$ Hz, 1H), 7.23 (s, 1H), 5.02–5.00 (m, 2H), 1.25–1.09 (m, 12H); ^{13}C NMR (100 MHz, CDCl_3) δ 161.2, 156.0, 146.6, 146.3, 144.5, 135.0, 132.7, 130.7, 126.9, 126.7, 126.5, 125.9, 123.7, 120.7, 120.0, 118.3, 70.9, 70.0, 22.0; HRMS (ESI⁺) m/z [M + H]⁺ calcd for $\text{C}_{24}\text{H}_{26}\text{BrN}_4\text{O}_5$: 529.1081, Found: 529.1077.

3fa. yellow solid (40.2 mg, 83%), $R_f = 0.32$ (25% EtOAc in hexane), mp 218.0–219.5 °C; ^1H NMR (400 MHz, CDCl_3) δ 10.40 (s, 1H), 8.33 (d, $J = 7.70$ Hz, 1H), 8.28 (d, $J = 7.48$ Hz, 1H), 8.06 (d, $J = 8.52$ Hz, 1H), 7.91 (t, $J = 7.76$ Hz, 1H), 7.76 (s, 1H), 7.65–7.55 (m, 3H), 7.24 (s, 1H), 5.02–4.99 (m, 2H), 1.26–1.10 (m, 12H); ^{13}C NMR (100 MHz, CDCl_3) δ 160.9, 156.1, 150.3, 150.1, 140.4, 135.4, 132.3, 130.7, 127.5, 127.1, 126.8, 126.7, 125.8, 123.7, 121.3, 120.8, 118.8, 70.9, 70.0, 22.0; HRMS (ESI⁺) m/z [M + H]⁺ calcd for $\text{C}_{24}\text{H}_{26}\text{ClN}_4\text{O}_5$: 485.1586, Found: 485.1582.

3ga. yellow solid (44.7 mg, 95%), $R_f = 0.32$ (25% EtOAc in hexane), mp 195.5–197.0 °C; ^1H NMR (400 MHz, CDCl_3) δ 10.28 (s, 1H), 8.35 (d, $J = 7.92$ Hz, 1H), 8.25 (dd, $J_1 = 1.48$ Hz, $J_2 = 7.36$ Hz, 1H), 8.07–8.01 (m, 3H), 7.75 (s, 1H), 7.64–7.57 (m, 2H), 7.32 (s, 1H), 7.19 (dd, $J_1 = 1.96$ Hz, $J_2 = 8.16$ Hz, 1H), 5.02–4.99 (m, 2H), 1.25–1.10 (m, 12H); ^{13}C NMR (100 MHz, CDCl_3) δ 162.0 (d, $J = 243.57$ Hz), 160.9, 156.1, 148.4 (d, $J = 10.63$ Hz), 143.0 (d, $J = 10.63$ Hz), 135.4, 132.2, 130.7, 127.0, 126.8, 126.7, 125.8, 123.8, 120.7, 120.3 (d, $J = 3.66$ Hz), 118.7, 113.2 (d, $J = 35.47$ Hz), 70.9, 70.0, 22.0; ^{19}F NMR (376 MHz, CDCl_3): δ -66.95 (s, 1F); HRMS (ESI⁺) m/z [M + H]⁺ calcd for $\text{C}_{24}\text{H}_{26}\text{FN}_4\text{O}_5$: 469.1882, Found: 469.1880.

3ha. pale yellow solid (43.1 mg, 89%), $R_f = 0.32$ (25% EtOAc in hexane), mp 170.6–172.4 °C; ^1H NMR (400 MHz, CDCl_3) δ 10.67 (s, 1H), 8.59 (d, $J = 5.24$ Hz, 1H), 8.38 (d, $J = 7.89$ Hz, 1H), 8.35 (d, $J = 1.80$ Hz, 1H), 8.09–8.04 (m, 2H), 7.75 (s, 1H), 7.62–7.56 (m, 2H), 7.52 (dd, $J_1 = 1.92$ Hz, $J_2 = 5.20$ Hz, 1H), 7.35 (s, 1H), 5.02–5.01 (m, 2H), 1.25–1.10 (m, 12H); ^{13}C NMR (100 MHz, CDCl_3) δ 161.0, 156.1, 151.3, 149.0, 146.4, 135.2, 132.3, 130.7, 126.8, 126.6, 125.9, 123.8, 123.2, 120.6, 118.3, 70.9, 70.0, 22.0, 21.9; HRMS (ESI⁺) m/z [M + H]⁺ calcd for $\text{C}_{24}\text{H}_{26}\text{ClN}_4\text{O}_5$: 485.1586, Found: 485.1583.

3ia. pale yellow solid (45.0 mg, 97%), $R_f = 0.32$ (25% EtOAc in hexane), mp 192.1–194.0 °C; ^1H NMR (400 MHz, CDCl_3) δ 11.05 (s, 1H), 8.54 (d, $J = 3.81$ Hz, 1H), 8.37 (d, $J = 7.24$ Hz, 1H), 8.11–8.08 (m, 2H), 7.73 (s, 1H), 7.67 (d, $J = 7.64$ Hz, 1H), 7.61–7.55 (m, 2H), 7.40 (q, $J = 7.74$ Hz, 1H), 7.23 (s, 1H), 5.02–5.00 (m, 2H), 2.85 (s, 3H), 1.25–1.09 (m, 12H); ^{13}C NMR (100 MHz, CDCl_3) δ 163.7, 156.0, 146.7, 145.5, 141.4, 136.4, 134.6, 133.1, 130.7, 127.1, 126.6, 126.3, 126.2, 126.0, 123.6, 121.0, 118.0, 70.8, 69.9, 22.0, 20.8; HRMS (ESI⁺) m/z $[\text{M} + \text{K}]^+$ calcd for $\text{C}_{25}\text{H}_{28}\text{N}_4\text{O}_5\text{K}$: 503.1691, Found: 503.1691.

3ga. yellow solid (32.6 mg, 70%), $R_f = 0.32$ (25% EtOAc in hexane), mp 202.5–204.4 °C; ^1H NMR (400 MHz, CDCl_3) δ 10.89 (s, 1H), 8.42 (d, $J = 7.57$ Hz, 1H), 8.17–8.08 (m, 3H), 7.83–7.73 (m, 2H), 7.64–7.56 (m, 2H), 7.37 (d, $J = 7.68$ Hz, 1H), 7.26 (s, 1H), 5.02–4.99 (m, 2H), 2.70 (s, 3H), 1.37–1.00 (m, 12H); ^{13}C NMR (100 MHz, CDCl_3) δ 162.4, 157.2, 156.1, 149.1, 137.9, 134.8, 132.8, 130.8, 126.9, 126.7, 126.4, 126.4, 126.0, 123.7, 120.8, 119.6, 118.1, 70.8, 70.0, 24.4, 22.0; HRMS (ESI⁺) m/z $[\text{M} + \text{K}]^+$ calcd for $\text{C}_{25}\text{H}_{28}\text{N}_4\text{O}_5\text{K}$: 503.1691, Found: 503.1690.

3ka. yellow solid (32.3 mg, 67%), $R_f = 0.32$ (25% EtOAc in hexane), mp 191.0–192.5 °C; ^1H NMR (400 MHz, CDCl_3) δ 10.57 (s, 1H), 8.68 (d, $J = 4.20$ Hz, 1H), 8.36 (d, $J = 7.80$ Hz, 1H), 8.28 (d, $J = 8.00$ Hz, 1H), 8.05 (s, 1H), 7.94 (dt, $J_1 = 1.55$ Hz, $J_2 = 9.26$ Hz, 1H), 7.57–7.51 (m, 2H), 7.33 (d, $J = 2.88$ Hz, 1H), 7.26–7.23 (m, 2H), 5.02–4.99 (m, 2H), 3.96 (s, 3H), 1.29–1.09 (m, 12H); ^{13}C NMR (100 MHz, CDCl_3) δ 162.3, 158.2, 156.0, 149.9, 148.2, 137.8, 135.3, 131.5, 128.6, 126.6, 126.2, 125.7, 123.2, 122.6, 119.6, 118.6, 100.4, 70.8, 69.9, 55.3, 22.0, 21.8; HRMS (ESI⁺) m/z $[\text{M} + \text{H}]^+$ calcd for $\text{C}_{25}\text{H}_{29}\text{N}_4\text{O}_6$: 481.2082, Found: 481.2081.

3la. yellow solid (37.5 mg, 80%), $R_f = 0.32$ (25% EtOAc in hexane), mp 175.9–177.6 °C; ^1H NMR (400 MHz, CDCl_3) δ 9.90 (s, 1H), 8.70 (d, $J = 4.20$ Hz, 1H), 8.33 (d, $J = 7.80$ Hz, 1H), 7.97–7.92 (m, 3H), 7.68 (s, 1H), 7.55–7.52 (m, 1H), 7.49–7.46 (m, 2H), 7.20 (s, 1H), 5.02–4.99 (m, 2H), 2.46 (s, 3H), 1.37–1.12 (m, 12H); ^{13}C NMR (100 MHz, CDCl_3) δ 162.9, 155.9, 149.6, 148.3, 137.6, 137.2, 133.2, 131.3, 130.3, 129.3, 128.6, 126.7, 126.6, 126.0, 123.0, 122.7, 70.9, 70.0, 22.0, 18.9; HRMS (ESI⁺) m/z $[\text{M} + \text{K}]^+$ calcd for $\text{C}_{25}\text{H}_{28}\text{N}_4\text{O}_5\text{K}$: 503.1691, Found: 503.1690.

3ma. yellow solid (47.5 mg, 88%), $R_f = 0.32$ (25% EtOAc in hexane), mp 113.6–115.0 °C; ^1H NMR (400 MHz, CDCl_3) δ 13.96 (s, 1H), 9.14 (d, $J = 8.50$ Hz, 1H), 8.73 (d, $J = 4.17$ Hz, 1H), 8.38 (d, $J = 7.84$ Hz, 1H), 7.95–7.72 (m, 3H), 7.54–7.47 (m, 2H), 7.41 (d, $J = 7.33$ Hz, 1H), 7.20 (s, 1H), 5.02–4.99 (m, 2H), 4.25 (s, 2H), 3.84 (s, 2H), 3.19–2.98 (m, 4H), 1.25–1.03 (m, 12H); ^{13}C NMR (100 MHz, CDCl_3) δ 163.4, 156.0, 151.0, 149.5, 147.9, 137.6, 135.9, 134.0, 133.0, 126.5, 126.4, 123.5, 120.4, 120.3, 117.3, 116.5, 70.8, 70.0, 65.5, 55.1, 54.3, 53.8, 22.0; HRMS (ESI⁺) m/z $[\text{M} + \text{K}]^+$ calcd for $\text{C}_{28}\text{H}_{33}\text{N}_5\text{O}_6\text{K}$: 574.2062, Found: 574.2059.

3na. yellow solid (26.7 mg, 50%), $R_f = 0.32$ (25% EtOAc in hexane), mp 221.6–223.5 °C; ^1H NMR (400 MHz, CDCl_3) δ 9.65 (s, 1H), 8.30 (d, $J = 7.88$ Hz, 1H), 8.16–8.07 (m, 3H), 7.80–7.73 (m, 2H), 7.56–7.52 (m, 1H), 7.42–7.28 (m, 5H), 7.19 (s, 2H), 7.01 (t, $J = 7.43$ Hz, 1H), 5.04–5.02 (m, 2H), 1.34–1.08 (m, 12H); ^{13}C NMR (100 MHz, CDCl_3) δ 161.9, 155.9, 149.5, 147.3, 142.4, 138.1, 137.0, 135.7, 433.4, 132.1, 130.9, 129.2, 128.1, 126.9, 125.8, 125.7, 125.4, 123.1, 121.8, 70.9, 70.0, 29.7, 22.0; HRMS (ESI⁺) m/z $[\text{M} + \text{K}]^+$ calcd for $\text{C}_{30}\text{H}_{30}\text{N}_4\text{O}_5\text{K}$: 565.1848, Found: 565.1847.

3oa. yellow solid (41.0 mg, 80%), $R_f = 0.32$ (25% EtOAc in hexane), mp 181.1–183.9 °C; ^1H NMR (400 MHz, CDCl_3) δ 10.67 (s, 1H), 8.65–8.64 (m, 1H), 8.36 (d, $J = 7.81$ Hz, 1H), 8.12 (d, $J = 7.33$ Hz, 1H), 7.94–7.90 (m, 2H), 7.75 (s, 1H), 7.51–7.48 (m, 1H), 7.39 (t, $J = 7.10$ Hz, 1H), 7.30 (d, $J = 6.88$ Hz, 1H), 5.01–4.99 (m, 2H), 2.99 (s, 3H), 1.25–1.03 (m, 12H); ^{13}C NMR (100 MHz, CDCl_3) δ 162.2, 156.0, 149.9, 148.2, 137.7, 136.4, 133.7, 133.1, 132.4, 130.5, 128.6, 126.5, 126.3, 125.6, 122.7, 121.9, 70.8, 69.9, 25.1, 22.0; HRMS (ESI⁺) m/z $[\text{M} + \text{K}]^+$ calcd for $\text{C}_{25}\text{H}_{28}\text{N}_4\text{O}_5\text{K}$: 503.1691, Found: 503.1688.

3pa. yellow solid (34.1 mg, 68%), $R_f = 0.32$ (25% EtOAc in hexane), mp 185.4–187.0 °C; ^1H NMR (400 MHz, CDCl_3) δ 11.02 (s, 1H), 8.47–8.37 (m, 3H), 8.26 (d, $J = 8.47$ Hz, 1H), 8.19 (d, $J = 8.33$ Hz, 1H), 8.11 (s, 1H), 7.92 (d, $J = 8.14$ Hz, 1H), 7.85–7.79 (m, 2H), 7.68–7.59 (m, 3H), 7.29 (s, 1H), 5.04–5.02 (m, 2H), 1.27–1.11 (m, 12H); ^{13}C NMR (100 MHz, CDCl_3) δ 162.4, 156.1, 149.6, 146.3, 138.0, 135.0, 132.8, 130.8, 130.4, 129.8, 129.5, 128.3, 127.8, 127.0, 126.7,

126.5, 126.0, 123.8, 120.8, 118.8, 118.2, 70.9, 70.0, 22.0; HRMS (ESI⁺) m/z [M + K]⁺ calcd for C₂₈H₂₈N₄O₅K: 539.1691, Found: 539.1690.

3qa. yellow solid (34.4 mg, 68%), R_f = 0.32 (25% EtOAc in hexane), mp 223.1–224.2 °C; ¹H NMR (400 MHz, CDCl₃) δ 11.16 (s, 1H), 9.78 (d, *J* = 7.92 Hz, 1H), 8.62 (d, *J* = 4.30 Hz, 1H), 8.44 (d, *J* = 7.26 Hz, 1H), 8.16–8.07 (m, 2H), 7.90 (d, *J* = 6.08 Hz, 2H), 7.77–7.71 (m, 3H), 7.63–7.57 (m, 2H), 7.20 (s, 1H), 5.02 (s, 1H), 1.26–1.06 (m, 12H); ¹³C NMR (100 MHz, CDCl₃) δ 163.8, 156.1, 147.3, 140.0, 137.7, 134.9, 133.1, 130.8, 130.7, 129.0, 127.8, 127.4, 127.2, 126.9, 126.7, 126.4, 126.0, 125.1, 123.6, 121.0, 118.3, 70.9, 70.0, 22.0, 21.9; HRMS (ESI⁺) m/z [M + K]⁺ calcd for C₂₈H₂₈N₄O₅K: 539.1691, Found: 539.1692.

3ab. pale yellow solid (29.8 mg, 73%), R_f = 0.32 (25% EtOAc in hexane), mp 81.2–83.9 °C; ¹H NMR (400 MHz, CDCl₃) δ 10.81 (s, 1H), 8.69–8.68 (m, 1H), 8.40 (d, *J* = 7.94 Hz, 1H), 8.34 (d, *J* = 7.81 Hz, 1H), 8.10–8.08 (m, 2H), 7.90 (dt, *J*₁ = 1.24 Hz, *J*₂ = 7.68 Hz, 1H), 7.78 (s, 1H), 7.58 (t, *J* = 6.99 Hz, 2H), 7.52–7.49 (m, 2H), 7.29–7.20 (m, 2H), 7.05 (s, 1H), 5.15 (s, 4H); ¹³C NMR (100 MHz, CDCl₃) δ 162.3, 156.1, 149.7, 148.1, 137.8, 135.7, 135.4, 134.4, 133.0, 130.6, 128.5, 128.2, 128.0, 127.6, 127.0, 126.8, 126.7, 126.6, 126.1, 123.6, 120.8, 118.0, 68.4, 67.8; HRMS (ESI⁺) m/z [M + H]⁺ calcd for C₃₂H₂₇N₄O₅: 547.1976, Found: 547.1973.

3cb. yellow solid (48.4 mg, 83%), R_f = 0.32 (25% EtOAc in hexane), mp 68.9–70.2 °C; ¹H NMR (400 MHz, CDCl₃) δ 10.55 (s, 1H), 8.61 (d, *J* = 2.12 Hz, 1H), 8.33 (d, *J* = 7.89 Hz, 1H), 8.26 (d, *J* = 8.33 Hz, 1H), 8.09–8.01 (m, 2H), 7.81–7.79 (m, 3H), 7.59–7.50 (m, 2H), 7.30–7.91 (m, 9H), 7.04 (s, 1H), 5.14 (s, 4H); ¹³C NMR (100 MHz, CDCl₃) δ 161.5, 156.2, 147.8, 147.2, 137.5, 135.7, 135.6, 135.5, 134.7, 132.7, 130.7, 128.5, 128.3, 128.2, 127.6, 127.0, 126.8, 126.7, 126.0, 123.8, 123.6, 120.7, 118.3, 68.4, 67.8; HRMS (ESI⁺) m/z [M + H]⁺ calcd for C₃₂H₂₆ClN₄O₅: 581.1586, Found: 581.1584.

3bd. pale yellow solid (58.6 mg, 94%), R_f = 0.32 (25% EtOAc in hexane), mp 69.4–71.6 °C; ¹H NMR (400 MHz, CDCl₃) δ 10.55 (s, 1H), 8.71 (d, *J* = 1.92 Hz, 1H), 8.32 (d, *J* = 7.93 Hz, 1H), 8.19–8.10 (m, 2H), 8.01 (d, *J* = 8.61 Hz, 1H), 7.94 (d, *J* = 7.72 Hz, 1H), 7.83–7.75 (m, 2H), 7.58–7.49 (m, 2H), 7.26–7.18 (m, 9H), 7.03 (s, 1H), 5.13 (s, 4H); ¹³C NMR (100 MHz, CDCl₃) δ 161.6, 156.2, 149.4, 148.2, 140.5, 135.7, 135.5, 134.8, 132.6, 130.7, 128.5, 128.3, 128.2, 128.1, 127.6, 127.0, 126.8, 126.7, 126.0, 124.6, 124.0, 123.8, 120.6, 118.3, 68.4, 67.8; HRMS (ESI⁺) m/z [M + H]⁺ calcd for C₃₂H₂₆BrN₄O₅: 625.1081 Found: 625.1080.

3eb. white solid (41.8 mg, 67%), R_f = 0.32 (25% EtOAc in hexane), mp 74.1–75.3 °C; ¹H NMR (400 MHz, CDCl₃) δ 10.74 (s, 1H), 8.63 (d, *J* = 4.05 Hz, 1H), 8.38 (d, *J* = 7.87 Hz, 1H), 8.10–8.01 (m, 3H), 7.76 (s, 1H), 7.58–7.50 (m, 3H), 7.34–7.72 (m, 10H), 7.05 (s, 1H), 5.15 (s, 4H); ¹³C NMR (100 MHz, CDCl₃) δ 161.1, 156.1, 146.5, 146.2, 144.5, 135.6, 135.4, 134.4, 132.9, 130.5, 128.5, 128.3, 128.1, 127.6, 126.9, 136.9, 126.6, 126.0, 123.5, 120.7, 120.0, 118.1, 68.4, 67.9; HRMS (ESI⁺) m/z [M + H]⁺ calcd for C₃₂H₂₆BrN₄O₅: 625.1081 Found: 625.1080.

3fb. pale yellow solid (41.9 mg, 72%), R_f = 0.32 (25% EtOAc in hexane), mp 75.9–77.3 °C; ¹H NMR (400 MHz, CDCl₃) δ 10.37 (s, 1H), 8.29–8.23 (m, 2H), 8.03 (d, *J* = 8.56 Hz, 2H), 7.84–7.70 (m, 3H), 7.60 (t, *J* = 7.05 Hz, 1H), 7.51 (d, *J* = 7.88 Hz, 2H), 7.28–7.20 (m, 9H), 7.04 (s, 1H), 5.14 (s, 4H); ¹³C NMR (100 MHz, CDCl₃) δ 161.0, 156.2, 150.2, 150.1, 140.4, 135.6, 135.4, 135.0, 132.5, 130.6, 128.5, 128.3, 128.2, 127.6, 127.5, 127.1, 126.8, 126.0, 123.7, 121.3, 120.8, 118.7, 68.4, 67.8; HRMS (ESI⁺) m/z [M + H]⁺ calcd for C₃₂H₂₆ClN₄O₅: 581.1586, Found: 581.1585.

3hb. pale yellow solid (46.7 mg, 80%), R_f = 0.32 (25% EtOAc in hexane), mp 70.5–71.1 °C; ¹H NMR (400 MHz, CDCl₃) δ 10.65 (s, 1H), 8.57 (d, *J* = 5.24 Hz, 1H), 8.36–8.33 (m, 2H), 8.03 (d, *J* = 8.66 Hz, 2H), 7.77 (s, 1H), 7.59–7.55 (m, 2H), 7.50 (dd, *J*₁ = 1.96 Hz, *J*₂ = 5.16 Hz, 2H), 7.30–7.20 (m, 9H), 7.04 (s, 1H), 5.14 (s, 4H); ¹³C NMR (100 MHz, CDCl₃) δ 161.1, 156.1, 151.2, 149.0, 146.4, 135.6, 135.4, 134.7, 132.7, 130.6, 128.5, 128.3, 128.2, 127.7, 127.0, 126.9, 126.7, 126.1, 123.6, 123.2, 120.7, 118.1, 68.5, 67.9; HRMS (ESI⁺) m/z [M + H]⁺ calcd for C₃₂H₂₆ClN₄O₅: 581.1586, Found: 581.1586.

3ib. white solid (44.7 mg, 80%), R_f = 0.32 (25% EtOAc in hexane), mp 67.1–69.5 °C; ¹H NMR (400 MHz, CDCl₃) δ 11.05 (s, 1H), 8.52 (d, *J* = 3.61 Hz, 1H), 8.35 (d, *J* = 7.92 Hz, 1H), 8.07 (d, *J* = 8.73 Hz, 2H), 7.75 (s, 1H), 7.65–7.49 (m, 4H), 7.38 (dd, *J*₁ = 4.46 Hz, *J*₂ = 7.72 Hz, 2H), 7.28–7.20 (m, 8H), 7.05 (s, 1H), 5.14 (s, 4H), 2.82 (s, 3H); ¹³C NMR (100 MHz, CDCl₃)

δ 163.8, 156.1, 146.7, 145.5, 141.4, 136.4, 135.7, 135.5, 134.1, 133.5, 130.6, 128.5, 128.3, 128.2, 127.6, 127.1, 126.9, 126.5, 126.2, 123.5, 121.1, 117.8, 68.4, 67.8, 20.8; HRMS (ESI⁺) m/z [M + K]⁺ calcd for C₃₃H₂₈N₄O₅K: 599.1691, Found: 599.1692.

3ac. pale yellow solid (45.8 mg, 95%), R_f = 0.32 (25% EtOAc in hexane), mp 215.5–216.8 °C; ¹H NMR (400 MHz, CDCl₃) δ 10.80 (s, 1H), 8.69 (d, J = 4.28 Hz, 1H), 8.43 (d, J = 7.29 Hz, 1H), 8.34 (d, J = 7.77 Hz, 1H), 8.10–8.08 (m, 2H), 7.92 (t, J = 7.26 Hz, 1H), 7.73 (s, 1H), 7.59–7.57 (m, 2H), 7.51 (t, J = 6.04 Hz, 1H), 7.11 (s, 1H), 1.48–1.25 (m, 18H); ¹³C NMR (100 MHz, CDCl₃) δ 162.2, 155.5, 149.9, 148.1, 137.8, 135.6, 132.4, 130.7, 126.6, 126.3, 123.9, 122.5, 120.7, 118.0, 82.0, 81.3, 28.2, 28.0; HRMS (ESI⁺) m/z [M + H]⁺ calcd for C₂₆H₃₁N₄O₅: 479.2289, Found: 479.2288.

3cc. white solid (25.8 mg, 50%), R_f = 0.32 (25% EtOAc in hexane), mp 170.1–172.2 °C; ¹H NMR (400 MHz, CDCl₃) δ 10.56 (s, 1H), 8.65 (d, J = 2.12 Hz, 1H), 8.38 (d, J = 7.54 Hz, 1H), 8.31 (d, J = 8.32 Hz, 1H), 8.06–8.04 (m, 2H), 7.92 (dd, J_1 = 2.17 Hz, J_2 = 8.33 Hz, 1H), 7.22 (s, 1H), 7.62–7.57 (m, 2H), 7.00 (s, 1H), 1.49–1.30 (m, 18H); ¹³C NMR (100 MHz, CDCl₃) δ 161.3, 155.4, 148.0, 147.2, 137.5, 135.7, 135.5, 132.0, 130.7, 126.7, 126.6, 126.4, 125.9, 125.5, 123.9, 123.6, 120.6, 118.2, 82.1, 81.4, 29.6, 28.2, 28.0; HRMS (ESI⁺) m/z [M + H]⁺ calcd for C₂₆H₃₀ClN₄O₅: 513.1899, Found: 513.1901.

3dc. pale yellow solid (29.4 mg, 53%), R_f = 0.32 (25% EtOAc in hexane), mp 182.7–184.9 °C; ¹H NMR (400 MHz, CDCl₃) δ 10.57 (s, 1H), 8.77 (d, J = 1.95 Hz, 1H), 8.38 (d, J = 7.58 Hz, 1H), 8.24 (d, J = 8.41 Hz, 1H), 8.09–8.04 (m, 3H), 7.73 (s, 1H), 7.62–7.57 (m, 2H), 6.99 (s, 1H), 1.55–1.30 (m, 18H); ¹³C NMR (100 MHz, CDCl₃) δ 161.5, 154.8, 149.4, 148.4, 140.5, 135.7, 132.0, 130.7, 126.7, 126.4, 125.4, 124.5, 123.9, 120.6, 118.2, 82.1, 81.4, 29.6, 28.2, 28.0; HRMS (ESI⁺) m/z [M + H]⁺ calcd for C₂₆H₃₀BrN₄O₅: 557.1394, Found: 557.1395.

3fc. pale yellow solid (34.8 mg, 68%), R_f = 0.32 (25% EtOAc in hexane), mp 207.8–209.6 °C; ¹H NMR (400 MHz, CDCl₃) δ 10.39 (s, 1H), 8.33 (d, J = 7.78 Hz, 1H), 8.27 (d, J = 7.35 Hz, 1H), 8.05 (d, J = 8.80 Hz, 2H), 7.90 (t, J = 7.79 Hz, 1H), 7.73 (s, 1H), 7.64–7.57 (m, 2H), 7.55 (d, J = 7.78 Hz, 1H), 7.05 (s, 1H), 1.48–1.25 (m, 18H); ¹³C NMR (100 MHz, CDCl₃) δ 160.9, 155.5, 154.7, 150.4, 150.1, 140.4, 136.0, 131.9, 130.7, 127.4, 127.0, 126.6, 125.3, 123.9, 121.2, 120.7, 118.8, 82.1, 82.5, 28.2, 28.0; HRMS (ESI⁺) m/z [M + Na]⁺ calcd for C₂₆H₂₉ClN₄O₅Na: 535.1719, Found: 535.1724.

3ic. yellow solid (39.5 mg, 80%), R_f = 0.32 (25% EtOAc in hexane), mp 197.0–198.1 °C; ¹H NMR (400 MHz, CDCl₃) δ 11.04 (s, 1H), 8.54–8.53 (m, 1H), 8.37 (d, J = 7.09 Hz, 1H), 8.10–8.07 (m, 2H), 7.70–7.65 (m, 2H), 7.59–7.55 (m, 2H), 7.40 (dd, J_1 = 4.58 Hz, J_2 = 7.70 Hz, 1H), 7.03 (s, 1H), 2.85 (s, 3H), 1.48–1.25 (m, 18H); ¹³C NMR (100 MHz, CDCl₃) δ 163.7, 155.4, 146.8, 145.5, 141.4, 136.3, 135.2, 132.8, 130.7, 127.0, 126.4, 126.2, 126.2, 123.7, 121.0, 118.0, 82.0, 81.3, 28.2, 28.0, 20.8; HRMS (ESI⁺) m/z [M + H]⁺ calcd for C₂₇H₃₃N₄O₅: 493.2445, Found: 493.2446.

3jc. yellow solid (38.7 mg, 78%), R_f = 0.32 (25% EtOAc in hexane), mp 201.3–203.8 °C; ¹H NMR (400 MHz, CDCl₃) δ 10.83 (s, 1H), 8.41 (d, J = 7.48 Hz, 1H), 8.15 (d, J = 7.62 Hz, 1H), 8.09–8.07 (m, 2H), 7.81 (t, J = 7.68 Hz, 1H), 7.73 (s, 1H), 7.37 (d, J = 7.65 Hz, 1H), 7.06 (s, 1H), 2.70 (s, 3H), 1.48–1.30 (m, 18H); ¹³C NMR (100 MHz, CDCl₃) δ 162.4, 157.2, 155.4, 149.1, 137.9, 132.5, 130.8, 126.9, 126.4, 126.3, 123.9, 120.7, 119.6, 118.1, 82.0, 81.4, 28.2, 28.0, 24.4; HRMS (ESI⁺) m/z [M + H]⁺ calcd for C₂₇H₃₂N₄O₅: 493.2445, Found: 493.2448.

3nc. yellow solid (20.9 mg, 38%), R_f = 0.32 (25% EtOAc in hexane), mp 201.5–203.3 °C; ¹H NMR (400 MHz, CDCl₃) δ 9.62 (s, 1H), 8.29 (d, J = 6.17 Hz, 1H), 8.16 (d, J = 3.91 Hz, 1H), 8.07 (d, J = 7.73 Hz, 2H), 7.77–7.73 (m, 2H), 7.54 (t, J = 7.21 Hz, 1H), 3.39–3.26 (m, 4H), 7.19 (s, 1H), 7.02–6.98 (m, 2H), 1.56–1.34 (m, 18H); ¹³C NMR (100 MHz, CDCl₃) δ 161.9, 154.9, 149.6, 147.3, 142.4, 138.0, 137.0, 136.2, 133.0, 132.1, 130.8, 129.1, 128.1, 126.8, 125.7, 125.5, 123.2, 121.8, 82.1, 81.4, 29.6, 28.2, 28.1; HRMS (ESI⁺) m/z [M + H]⁺ calcd for C₃₂H₃₅N₄O₅: 555.2602, Found: 555.2603.

3oc. yellow solid (40.8 mg, 83%), R_f = 0.32 (25% EtOAc in hexane), mp 202.5–204.7 °C; ¹H NMR (400 MHz, CDCl₃) δ 10.65 (s, 1H), 8.65 (d, J = 4.43 Hz, 1H), 8.35 (d, J = 7.82 Hz, 1H), 7.94–7.88 (m, 2H), 7.33–7.32 (m, 1H), 7.51–7.48 (m, 1H), 7.39 (t, J = 7.15 Hz, 1H), 7.29 (d, J = 6.91 Hz, 1H), 7.03 (s, 1H), 2.99 (s, 3H), 1.47–1.43 (m, 18H); ¹³C NMR (100 MHz, CDCl₃)

δ 162.2, 155.3, 154.9, 149.9, 148.1, 137.7, 137.0, 133.3, 133.0, 132.3, 130.3, 128.5, 126.5, 126.1, 125.2, 122.1, 82.0, 81.3, 28.2, 28.0, 25.1; HRMS (ESI⁺) m/z [M + H]⁺ calcd for C₂₇H₃₃N₄O₅: 493.2445, Found: 493.2443.

4. Conclusions

In summary, we developed a simple and efficient protocol for silver(I)-catalyzed amination of 1-naphthylamine derivatives with azodicarboxylate at the C4 site in acetone at room temperature, leading to the target products in mostly good yields. Note that this reaction might proceed with a self-redox process under external-oxidant and additive-free conditions. The reaction is compatible with a variety of functional groups on both the pyridine and naphthene rings of 1-naphthylamine derivatives.

Supplementary Materials: The following are available online at <https://www.mdpi.com/article/10.3390/catal12091006/s1>, Table S1: Optimization of Catalyst and Solvent, Table S2: Optimization of Catalyst Loading, Table S3: Optimization of Time.

Author Contributions: F.Y., Y.W. review and editing, and supervision. Y.Z., M.P. the main part of the experimental and data collection, writing—original draft preparation. All authors have read and agreed to the published version of the manuscript.

Funding: We are grateful to the National Natural Science Foundation of China (nos. 21172200, 21102134) for its financial support.

Data Availability Statement: The Supporting Information is available free of charge on the website. Experimental details.

Acknowledgments: The authors would like to thank Zhen Liu from East China University of Science and Technology for support in mechanistic calculation.

Conflicts of Interest: The authors declare no conflict of interest.

References

1. Horton, D.A.; Bourne, G.T.; Smythe, M.L. The Combinatorial Synthesis of Bicyclic Privileged Structures or Privileged Substructures. *Chem. Rev.* **2003**, *103*, 893–930. [CrossRef] [PubMed]
2. Lygaitis, R.; Getautis, V.; Grazulevicius, J.V. Hole-Transporting Hydrazones. *Chem. Soc. Rev.* **2008**, *37*, 770–788. [CrossRef] [PubMed]
3. Liang, M.; Chen, J. Arylamine Organic Dyes for Dye-Sensitized Solar Cells. *Chem. Soc. Rev.* **2013**, *42*, 3453–3488. [CrossRef] [PubMed]
4. Guram, A.S.; Rennels, R.A.; Buchwald, S.L. A Simple Catalytic Method for the Conversion of Aryl Bromides to Arylamines. *Angew. Chem. Int. Ed. Engl.* **1995**, *34*, 1348–1350. [CrossRef]
5. Louie, J.; Hartwig, J.F. Palladium-Catalyzed Synthesis of Arylamines from Aryl Halides. Mechanistic Studies Lead to Coupling in the Absence of Tin Reagents. *Tetrahedron Lett.* **1995**, *36*, 3609–3612. [CrossRef]
6. Zhang, C.; Tang, C.H.; Jiao, N. Recent Advances in Copper-Catalyzed Dehydrogenative Functionalization via a Single Electron Transfer (SET) Process. *Chem. Soc. Rev.* **2012**, *41*, 3464–3484. [CrossRef]
7. Ping, L.; Chung, D.S.; Bouffard, J.; Lee, S.G. Transition Metal-Catalyzed Site- and Regio-Divergent C-H Bond Functionalization. *Chem. Soc. Rev.* **2017**, *46*, 4299–4328. [CrossRef]
8. Yang, L.; Huang, H.M. Transition-Metal-Catalyzed Direct Addition of Unactivated C-H Bonds to Polar Unsaturated Bonds. *Chem. Rev.* **2015**, *115*, 3468–3517. [CrossRef]
9. Wei, Y.; Hu, P.; Zhang, M.; Su, W.P. Metal-Catalyzed Decarboxylative C-H Functionalization. *Chem. Rev.* **2017**, *117*, 8864–8907. [CrossRef]
10. Rej, S.; Ano, Y.; Chatani, N. Bidentate Directing Groups: An Efficient Tool in C-H Bond Functionalization Chemistry for the Expedient Construction of C-C Bonds. *Chem. Rev.* **2020**, *120*, 1788–1887. [CrossRef]
11. Large, B.; Prim, D. C-H Functionalization Strategies in the Naphthalene Series: Site Selections and Functional Diversity. *Synthesis* **2020**, *52*, 2600–2612.
12. Prevost, S. Regioselective C-H Functionalization of Naphthalenes: Reactivity and Mechanistic Insights. *ChemPlusChem* **2020**, *85*, 476–486. [CrossRef]
13. Zaitsev, V.G.; Shabashov, D.; Daugulis, O. Highly Regioselective Arylation of sp³ C-H Bonds Catalyzed by Palladium Acetate. *J. Am. Chem. Soc.* **2005**, *127*, 13154–13155. [CrossRef]
14. Xiao, Q.; Meng, X.T.; Kanai, M.; Kuninobu, Y. Palladium-Catalyzed C-H Fluorosilylation of 2-Phenylpyridines: Synthesis of Silafluorene Equivalents. *Angew. Chem. Int. Ed.* **2014**, *53*, 3168–3172. [CrossRef]
15. Xu, C.F.; Shen, Q.L. Palladium-Catalyzed Trifluoromethylthiolation of Aryl C-H Bonds. *Org. Lett.* **2014**, *16*, 2046–2049. [CrossRef]
16. Patel, P.; Chang, S. N-Substituted Hydroxylamines as Synthetically Versatile Amino Sources in the Iridium-Catalyzed Mild C-H Amidation Reaction. *Org. Lett.* **2014**, *16*, 3328–3331. [CrossRef]

17. Iwasaki, M.; Iyanaga, M.; Tsuchiya, Y.; Nishimura, Y.; Li, W.J.; Li, Z.P.; Nishihara, Y. Palladium-Catalyzed Direct Thiolation of Aryl C-H Bonds with Disulfides. *Chem. Eur. J.* **2014**, *20*, 2459–2462. [[CrossRef](#)]
18. Zhang, X.; Si, W.L.; Bao, M.; Asao, N.; Yamamoto, Y.; Jin, T.N. Rh(III)-Catalyzed Regioselective Functionalization of C-H Bonds of Naphthylcarbamates for Oxidative Annulation with Alkynes. *Org. Lett.* **2014**, *16*, 4830–4833. [[CrossRef](#)]
19. Kondrashov, M.; Raman, S.; Wendt, O.F. Metal Controlled Regioselectivity in the Cyclometallation of 2-(1-Naphthyl)Pyridine. *Chem. Commun.* **2015**, *51*, 911–913. [[CrossRef](#)]
20. Yang, Q.L.; Wang, X.Y.; Lu, J.Y.; Zhang, L.P.; Fang, P.; Mei, T.S. Copper-Catalyzed Electrochemical C-H Amination of Arenes with Secondary Amines. *J. Am. Chem. Soc.* **2018**, *140*, 11487–11494. [[CrossRef](#)]
21. Begam, H.M.; Choudhury, R.; Behera, A.; Jana, R. Copper-Catalyzed Electrophilic ortho C(sp²)-H Amination of Aryl Amines: Dramatic Reactivity of Bicyclic System. *Org. Lett.* **2019**, *21*, 4651–4656. [[CrossRef](#)] [[PubMed](#)]
22. Shang, R.; Iliyes, L.; Nakamura, E. Iron-Catalyzed Directed C(sp²)-H and C(sp³)-H Functionalization with Trimethylaluminum. *J. Am. Chem. Soc.* **2015**, *137*, 7660–7663. [[CrossRef](#)] [[PubMed](#)]
23. Guan, D.H.; Han, L.; Wang, L.L.; Song, H.; Chu, W.Y.; Sun, Z.Z. Direct Cyanation of Picolinamides Using K₄[Fe(CN)₆] as the Cyanide Source. *Chem. Lett.* **2015**, *44*, 743–745. [[CrossRef](#)]
24. Li, Z.X.; Sun, S.Y.; Qiao, H.J.; Yang, F.; Zhu, Y.; Kang, J.X.; Wu, Y.S.; Wu, Y.J. Palladium-Catalyzed Regioselective C8-H Amination of 1-Naphthylamine Derivatives with Aliphatic Amines. *Org. Lett.* **2016**, *18*, 4594–4597. [[CrossRef](#)]
25. Lan, J.Y.; Xie, H.S.; Lu, X.X.; Deng, Y.F.; Jiang, H.F.; Zeng, W. Co(II)-Catalyzed Regioselective Cross-Dehydrogenative Coupling of Aryl C-H Bonds with Carboxylic Acids. *Org. Lett.* **2017**, *19*, 4279–4282. [[CrossRef](#)]
26. Rej, S.; Chatani, N. Rhodium(I)-Catalyzed C8-Alkylation of 1-Naphthylamide Derivatives with Alkenes through a Bidentate Picolinamide Chelation System. *ACS Catal.* **2018**, *8*, 6699–6706. [[CrossRef](#)]
27. Xiong, Y.S.; Yu, Y.; Weng, J.; Lu, G. Copper-Catalyzed Peri-Selective Direct Sulfonylation of 1-Naphthylamines with Disulfides. *Org. Chem. Front.* **2018**, *5*, 982–989. [[CrossRef](#)]
28. Roy, S.; Pradhan, S.; Punniyamurthy, T. Copper-Mediated Regioselective C-H Etherification of Naphthylamides with Arylboronic Acids Using Water as an Oxygen Source. *Chem. Commun.* **2018**, *54*, 3899–3902. [[CrossRef](#)]
29. Yu, X.M.; Yang, F.; Wu, Y.S.; Wu, Y.J. Palladium-Catalyzed C8-H Acylation of 1-Naphthylamines with Acyl Chlorides. *Org. Lett.* **2019**, *21*, 1726–1729. [[CrossRef](#)]
30. Li, J.M.; Wang, Y.H.; Yu, Y.; Wu, R.B.; Weng, J.; Lu, G. Copper-Catalyzed Remote C-H Functionalizations of Naphthylamides through a Coordinating Activation Strategy and Single-Electron-Transfer (SET) Mechanism. *ACS Catal.* **2017**, *7*, 2661–2667. [[CrossRef](#)]
31. Bai, P.R.; Sun, S.Y.; Li, Z.X.; Qiao, H.J.; Su, X.X.; Yang, F.; Wu, Y.S.; Wu, Y.J. Ru/Cu Photoredox or Cu/Ag Catalyzed C4-H Sulfonylation of 1-Naphthylamides at Room Temperature. *J. Org. Chem.* **2017**, *82*, 12119–12127. [[CrossRef](#)]
32. Liang, S.; Bolte, M.; Mano-likakes, G. Copper-Catalyzed Remote para-C-H Functionalization of Anilines with Sodium and Lithium Sulfinates. *Chem. Eur. J.* **2017**, *23*, 96–100. [[CrossRef](#)]
33. Zhu, H.M.; Sun, S.Y.; Qiao, H.J.; Yang, F.; Kang, J.X.; Wu, Y.S.; Wu, Y.J. Silver(I)-Catalyzed C4-H Amination of 1-Naphthylamine Derivatives with Azodicarboxylates. *Org. Lett.* **2018**, *20*, 620–623. [[CrossRef](#)]
34. You, G.R.; Wang, K.; Wang, X.D.; Wang, G.D.; Sun, J.; Duan, G.Y.; Xia, C.C. Visible-Light-Mediated Nickel(II)-Catalyzed C-N Cross-Coupling in Water: Green and Regioselective Access for the Synthesis of Pyrazole-Containing Compounds. *Org. Lett.* **2018**, *20*, 4005–4009. [[CrossRef](#)]
35. Xu, J.; Du, K.; Shen, J.B.; Shen, C.; Chai, K.J.; Zhang, P.F. Copper(II)-Catalyzed Selective Para Amination of Arylamine with Pyrazole by C-H Functionalization. *ChemCatChem* **2018**, *10*, 3675–3679. [[CrossRef](#)]
36. Pei, M.X.; Zu, C.H.; Liu, Z.; Yang, F.; Wu, Y.J. Merging Photoredox Catalysis with Transition Metal Catalysis: Direct C4-H Sulfamidation of 1 Naphthylamine Derivatives. *J. Org. Chem.* **2021**, *86*, 11324–11332. [[CrossRef](#)]
37. Zhao, L.X.; Sun, M.M.; Yang, F.; Wu, Y.J. Silver(I) Promoted the C4-H Bond Phosphonation of 1-Naphthylamine Derivatives with H-Phosphonates. *J. Org. Chem.* **2021**, *86*, 11519–11530. [[CrossRef](#)]
38. Sahoo, T.; Sen, C.; Singh, H.; Suresh, E.; Ghosh, S.C. Copper-Catalyzed C4 Carboxylation of 1-Naphthylamide Derivatives with CBr₄/MeOH. *Adv. Synth. Catal.* **2019**, *361*, 3950–3957. [[CrossRef](#)]
39. Kumar, S.; Pradhan, S.; Roy, S.; De, P.B.; Punniyamurthy, T. Iron-Catalyzed Regioselective Remote C(sp²)-H Carboxylation of Naphthyl and Quinoline Amides. *J. Org. Chem.* **2019**, *84*, 10481–10489. [[CrossRef](#)] [[PubMed](#)]
40. Xu, X.B.; Chu, Z.Z.; Xia, C.C. Transition-Metal Free Oxidative C-H Etherification of Acylanilines with Alcohols through a Radical Pathway. *Org. Biomol. Chem.* **2019**, *17*, 6346–6350. [[CrossRef](#)] [[PubMed](#)]
41. Qiao, H.J.; Sun, S.Y.; Yang, F.; Zhu, Y.; Zhu, W.G.; Dong, Y.X.; Wu, Y.S.; Kong, X.T.; Jiang, L.; Wu, Y.J. Copper(I)-Catalyzed Sulfonylation of 8-Aminoquinoline Amides with Sulfonyl Chlorides in Air. *Org. Lett.* **2015**, *17*, 6086–6089. [[CrossRef](#)]
42. Sun, M.M.; Sun, S.Y.; Qiao, H.J.; Yang, F.; Zhu, Y.; Kang, J.X.; Wu, Y.S.; Wu, Y.J. Silver(I)-Promoted C5-H Phosphonation of 8-Aminoquinoline Amides with H-Phosphonates. *Org. Chem. Front.* **2016**, *3*, 1646–1650. [[CrossRef](#)]
43. Qiao, H.J.; Sun, S.Y.; Yang, F.; Zhu, Y.; Kang, J.X.; Wu, Y.S.; Wu, Y.J. Merging Photoredox Catalysis with Iron(III) Catalysis: C5-H Bromination and Iodination of 8-Aminoquinoline Amides in Water. *Adv. Synth. Catal.* **2017**, *359*, 1976–1980. [[CrossRef](#)]
44. Qiao, H.J.; Sun, S.Y.; Zhang, Y.; Zhu, H.M.; Yu, X.M.; Li, Z.X.; Yang, F.; Wu, Y.S.; Wu, Y.J. Merging Photoredox Catalysis with Transition Metal Catalysis: Site-Selective C4 or C5-H Phosphonation of 8-Aminoquinoline Amides. *Org. Chem. Front.* **2017**, *4*, 1981–1986. [[CrossRef](#)]